Published in final edited form as:
Microporous Mesoporous Mater. 2012 May 12; 153: 166–170. doi:10.1016/j.micromeso.2011.12.005.

Enzymatic conversion of CO_2 to bicarbonate in functionalized mesoporous silica

Yuehua Yu[1], **Baowei Chen**[1], **Wen Qi**[1,2], **Xiaolin Li**[1], **Yongsoon Shin**[1], **Chenghong Lei**[1,*], and **Jun Liu**[1]

[1]Pacific Northwest National Laboratory, Richland, WA 99352, USA

[2]School of Material Science and Engineering, Tianjin University, Tianjin 300072, P. R. China

Abstract

We report here a concept converting carbon dioxide to biocarbonate in a biomimetic nanoconfiguration. Carbonic anhydrase (CA), the fastest enzyme that can covert carbon dioxide to bicarbonate, can be spontaneously entrapped in carboxylic acid group-functionalized mesoporous silica (HOOC-FMS) with super-high loading density (up to 0.5 mg of protein/mg of FMS) in sharp contrast to normal porous silica. The binding of CA to HOOC-FMS resulted in a partial conformational change comparing to the enzyme free in solution, but it can be overcome with increased protein loading density. The higher the protein loading density, the less conformational change, hence the higher enzymatic activity and the higher enzyme immobilization efficiency (up to >60%). The released enzyme still displayed the native conformational structure and the same high enzymatic activity as that prior to the enzyme entrapment, indicating that the conformational change resulted from the electrostatic interaction of CA with HOOC-FMS was not permanent. This work may provide a new approach converting carbon dioxide to biocarbonate that can be integrated with the other part of biosynthesis process for the assimilation of carbon dioxide.

Keywords

carbonic anhydrase; functionalized mesopoorous silica; enzymatic activity; carbon dioxide; biocarbonate

Introduction

With the emerging greenhouse gas crisis, biomimetic carbon dioxide (CO_2) conversion has attracted intense interests [1–3]. In fact, the assimilation of CO_2 into organic material is among the most important biosynthesis processes [4–7]. The carbonic anhydrases (CA) can catalyze the rapid conversion of carbon dioxide to bicarbonate and play a key role in CO_2 transfer for cell respiration and photosynthesis [8–13]. The reaction rate of carbonic anhydrase is one of the fastest of all enzymes [14]. In those biosynthesis processes, CO_2 concentration and conversion of CO_2 to bicarbonate catalyzed by CA are usually among the first essential steps [4–7]. For example, both cyanobacteria and chemoautotrophic bacteria have a proteinaceous cellular micro-compartment called carboxysome containing large

Correspondence should be addressed to: chenghong.lei@pnl.gov; Tel: 1-509-3716962; Fax: 1-509-3717304.

amount of ribulose-1,5-bisphosphate carboxylase (Rubisco) and carbonic anhydrase (CA). In the carboxysome, Rubisco acts by fixing atmospheric CO_2 to the ribulose-1,5 bisphosphate to form 2 molecules of 3-phosphoglycerate [6], where CA can result in an approximate 1000-fold concentration of the inorganic carbon ($[CO_2] + [HCO_3^-]$) [7]. Importantly, in animals, the primary function of CA is to interconvert carbon dioxide and bicarbonate to maintain acid-base balance in tissues, and to help transport carbon dioxide out of tissues [15].

Confinement theory and modeling efforts have predicted that a protein or protein-substrate complex inside a confined space would be stabilized by folding forces not present for proteins in bulk solutions [16–18]. Mesoporous silicas have a surface area of up to 1000 $m^2 g^{-1}$ with ordered pore surface accounting for >95%. The proteins can be spontaneously entrapped in functionalized mesoporous silica (FMS) with rigid, uniform, open nanopore geometry in tens of nanometers via non-covalent interactions. FMS can also protect the proteins because the pore size is sufficiently small to eliminate any invading bacteria. Recent advances show that functionalized mesoporous silica (FMS) with high affinity for entrapping a protein can provide a confined and favorably interactive nanoenvironment that can maintain high level of protein activity and allow large amounts of protein loading compared to unfunctionalized mesoporous silica (UMS) or normal porous silica (NPS), where NPS had the non-open pore structure and the same average pore size but over a wide distribution range [19–30].

In this work, we propose to entrap carbonic anhydrase in FMS as a confined space partially mimicking the cellular environment and thereby converting CO_2 to bicarbonate in a functionalized nanoporous support. Bovine carbonic anhydrase II (CA) is selected within carbonic anhyrase family due to its high turnover number. We found that CA can be spontaneously loaded in carboxylic acid functionalized FMS with super-high loading density (up to 0.5 mg/mg of FMS), and the enzyme specific activity displayed higher activity with increasing protein loading density.

Materials and methods

Preparation of FMS-enzyme composites

The original unfunctionalized mesoporous silica (UMS), prepared by using non-ionic block copolymer surfactant as the template, had a pore size of 30 nm measured by the Barrett-Joyner-Halenda method, while the surface area was as great as 533 m^2/g with an average bead size of 12–15 μm [31, 32]. Normal porous silica (NPS) is unfunctionalized silica bulk material from PolyLC Inc., USA, item #BMSI 1203, which is normally used as the media material for chromatography. NPS has an average 12 μm bead size, an average 30 nm pore size over a wide distribution range, and a total surface area of ~100 m^2/g. A controlled hydration and condensation reaction was used to introduce functional groups into UMS or NPS [31, 32]. Coverage of 2% (or 20%) HOOC-FMS, HO_3S-FMS or NH_2-FMS means 2% (or 20%) of the total available silanol groups (5×10^{18} silanol groups per square meter) of UMS would be silanized with trimethoxysilane with the functional group HOOC, HO_3S or NH_2 [31, 32].

To prepare FMS-enzyme composites, 0.6–2.0 mg FMS with different functional groups were incubated with 70–1000 μL of 2.0 mg/mL bovine carbonic anhydrase isozyme II (CA, lyophilized powder) in deionzied water (pH 6.5) for 2 hours at 21±1 °C under 1,200 rpm shaking. The resulted suspension was centrifuged at 16,000 rpm at 4 °C and the FMS-enzyme composites were thoroughly rinsed with deionized water for at least 5 times. The collected supernatant in each rinsing circle was measured using a *Bradford* Assay Kit to make sure all non-tightly bound proteins were rinsed off. Protein loading density (P_{LD}) was

calculated by subtracting the total unbound proteins from the initial CA amount used for the incubation.

Enzyme activity measurement

Enzymatic activity of CA was measured according to the protocol provided by Sigma-Aldrich. In brief, 6.0 mL of pH 8.3, 20 mM Tris-H_2SO_4 buffer was placed on ice bath and 100 μL of ~0.01 mg/mL CA (or the CA entrapped in FMS) solution was added, followed with 4 mL of carbon dioxide-saturated solution. One unit will cause the pH of the 20 mM Tris-H_2SO_4 buffer to drop from 8.3 to 6.3 per minute at 0°C.

Fluorescence Spectroscopy

Fluorescence spectra was measured with Horiba Fluorolog-2 spectrometer at a protein concentration of 0.02 mg/mL. The emission spectra were taken from 300 to 450 nm with excitation wavelength at 285 nm. The excitation and emission slits width were 5 nm. The ratio of emission intensities at 332 and 352 nm was recorded after blank subtraction without normalization.

Circular Dichroism Spectroscopy

Ellipticity measurements were made on an Aviv 410 spectrometer at 200–260 nm range in a quartz cuvette with 10 mm path length under stirring at a protein concentration of 0.07 mg/mL. Each sample was scanned 3 times at a speed of 12 nm/min with step size of 0.2 nm. Information about amount of α helix, parallel, antiparallel, β-sheet and random coil was determined by deconvolution software CDNN 2.1.

Results and Discussion

We used FMS with large pores thereby yielding super-high protein loading density. Figure 1A shows the transmission electron microscopy (TEM) images of 20% HOOC-FMS resulted from 30 nm UMS. Unlike 3-nm and 10-nm mesoporous silica, the 30-nm mesoporous silica has a large degree of disordering [33], but it still reveals more or less uniform cage-like porous structure [34]. Figure 1B shows the protein structure of CA with surface charge distribution and its catalytic reaction.

The positive charges of a protein are attributable to a surplus of surface amino residues in lysines, arginines and/or histidines, while negative charges are caused by carboxylic residues in glutamates and/or aspartates. The functional groups of HOOC, HO_3S, and NH_2 would offer electrostatic, H-bond and hydrophilic interaction with the charged amino acid residues of protein molecules to facilitate protein entrapment. In this work, FMS was incubated in the enzyme stock solution, thereby avoiding harsh immobilization conditions. UMS and NPS were tested under the same conditions. The protein amount (mg) of an enzyme immobilized with one mg of a porous silica support is defined as the protein loading density, P_{LD}, and the corresponding activity (units) of the enzyme immobilized with one mg of a porous silica as the activity loading density (A_{LD}). The immobilization efficiency (I_e) is defined as the ratio of the specific activity of the immobilized enzyme (A_{LD}/P_{LD}) to the specific activity of the free enzyme in stock solution. Figure 1C shows P_{LD} of CA entrapped in various FMS in H_2O at 21±1 °C. P_{LD} was 0.46 and 0.49 mg/mg of FMS for 2% and 20% HOOC-FMS, respectively. P_{LD} was 0.27 and 0.21 mg/mg of FMS for 2% and 20% HO_3S-FMS, respectively. Comparing to P_{LD} of CA in UMS (0% HOOC-FMS), there were the dramatic increases of P_{LD} of CA in HOOC-FMS. In contrast, P_{LD} of CA in 2% and 20% NH_2-FMS was only 0.07 and 0.01 mg/mg of FMS, respectively. The results demonstrated that CA was entrapped with much higher P_{LD} in negatively-charged HOOC-FMS and HO_3S-FMS than that in positively-charged NH_2-FMS. The CA in UMS displayed a P_{LD} of 0.16 mg/mg,

which is more or less close to that in the negatively-charged FMS (HOOC- and HO_3S-) due to the silanol groups of UMS. The much higher P_{LD} of CA in the negatively-charged FMS comparing to that in the positively-charged FMS suggests that the electrostatic interaction was dominant in between CA and FMS. We believe that the positively-charged region of CA protein molecules was oriented to bind to the wall of the negatively-charged FMS, although CA has a pI value at 5.9 presenting an overall slightly negatively-charged state in H_2O (pH 6.5). As expected, because of its low surface area and non-open pore structure with wide pore size distribution, NPS (whether functionalized or not) exhibited substantially lower P_{LD} than HOOC- and HO_3S-FMS for CA (Figure 1C). We believe that, it was the large surface area, mesoporous structure, functionalization and electrostatic interaction that resulted in the high P_{LD} of CA in FMS.

The dominant electrostatic interaction of CA with HOOC-FMS was also confirmed by incubating FMS in the CA solutions at the different temperatures and with different pH and ionic strength. P_{LD} of CA with 20% HOOC-FMS in H_2O was increased from 0.49 mg/mg of FMS at 21±1 °C to 0.55 mg/mg of FMS at 14±1 °C because a lower temperature usually facilitates a stronger electrostatic binding. At 21±1 °C, although CA was more positively charged in 0.9% NaCl-H_2O solution (pH 5.6) than that in pure water, P_{LD} of CA in 20% HOOC-FMS in 0.9% NaCl-H_2O was decreased to 0.30 mg/mg of FMS due to the ionic effect of NaCl. When changing the incubation solution of CA from H_2O to pH 8.3, 20 mM Tris-H_2SO_4 buffer, P_{LD} of CA in 20% HOOC-FMS was dramatically decreased to 0.03 mg/mg of FMS.

Figure 2A shows that both A_{LD} and P_{LD} of CA entrapped in HOOC-FMS in H_2O were much higher than HOOC-NPS. P_{LD} of CA entrapped in 2% and 20% HOOC-FMS were 0.46 and 0.49 mg/mg of FMS and I_e were 49% and 62%, respectively. The results demonstrate that P_{LD} could be increased slightly but I_e can be improved further with the increased coverage of the functional groups. In sharp contrast, P_{LD} of CA with 2% and 20% HOOC-NPS were 0.10 and 0.08 mg/mg of FMS and I_e were 15.6% and 4.9%, respectively. Figure 2B shows that I_e of CA in 20% HOOC-FMS in H_2O was increased with increasing P_{LD}. The trend is very similar to that of organophosphorus hydrolase in HOOC-FMS due to the molecular crowding effect in the confined space [29]. Comparing to the lower loading density of CA on functionalized NPS with non-open pore structure, we believe that the higher loading density in the mesoporous structure resulted in higher I_e of CA in FMS.

To question whether there was any conformational change when CA was entrapped in HOOC-FMS, we compared the fluorescence and CD spectra of CA in HOOC-FMS and free CA in H_2O. It is well-known that intrinsic fluorescence of tyrosine (Tyr) and tryptophan (Trp) residues is sensitive to conformational change. Upon conformational change resulting in more Tyr and Trp exposure to aqueous solvent, fluorescence emission red shifts and intensity decreases, accompanying a decreasing ratio of fluorescence intensities at 332 and 352 nm (I_{332}/I_{352}), verse versa. This has been used to study CA structural change at various environments [35]. Figure 3A shows the fluorescence spectra of the free CA in H_2O, the entrapped CA in 20% HOOC-FMS, and the released CA from 20% HOOC-FMS in H_2O. Figure 3B shows the I_{332}/I_{352} ratio of the free CA and the CA entrapped in 20% HOOC-FMS at various P_{LD}. When P_{LD} of CA in HOOC-FMS was as low as 0.01 mg/mg of FMS (Figure 3A), its I_{332}/I_{352} ratio was 0.91, while the I_{332}/I_{352} ratio of the free CA was 0.99 (Figure 3B). This result indicates that at such a low level of P_{LD}, the electrostatic binding of CA to HOOC-FMS had resulted in the CA conformational change to some extent and accordingly more Tyr and Trp exposure to aqueous environment. Interestingly, the I_{332}/I_{352} ratio of CA in HOOC-FMS was ascending with the increase of P_{LD}, that is, the same trend of enzymatic activity (Figure 2). This means the higher the P_{LD}, the less exposure of Tyr and Trp residues to aqueous environment, hence the higher enzymatic activity (Figure 2B).

We believe that the higher P_{LD} of CA in HOOC-FMS might result in the molecular crowding effect [16–18], which lessened the conformational changes and accordingly less Tyr and Trp exposure. However, even I_e of CA in HOOC-FMS at the highest P_{LD} with the highest I_{332}/I_{352} ratio (up to 1.06) was just 62% (Figures 2 and 3B), indicating that the orientation of CA in HOOC-FMS was not in a perfect state allowing the substrate access and the product diffusion [29]. It is noteworthy that the released CA from HOOC-FMS displayed similar fluorescence spectra to that of the free CA prior to the entrapment, indicating that the electrostatic interaction of CA with HOOC-FMS did not induce permanent change on the CA protein structure. This is in agreement with that the specific activity of the released CA (3425.6 units/mg) from HOOC-FMS was ~95.6% of that of the free CA (3583.3 units/mg) prior to the entrapment.

To further study the interaction of CA with HOOC-FMS, we also tried to measure the CD spectra of the free CA in H_2O, the entrapped CA in 20% HOOC-FMS, and the released CA from 20% HOOC-FMS in H_2O. Although the CA entrapped in HOOC-FMS presents minimum CD signal, the released CA from HOOC-FMS has a similar profile and intensity as that of free CA in the same buffer (Figure 4A). CDNN analysis shows that the free CA and the released CA have very similar protein structure in terms of α-Helix, parallel, anti-parallel, β-sheet and random coil contents (Figure 4B). Therefore, the conformational change resulted from the electrostatic interaction of CA with HOOC-FMS was not permanent, which has been confirmed by the fluorescence spectra and the enzymatic activity measurement as described above.

Besides the H-bond and hydrophilic, and the dominant electrostatic interactions with FMS, CA with hydrophobic regions may also have the hydrophobic interaction with the spacers (carbon chains: $-CH_2-CH_2-$, $-CH_2-CH_2-CH_2-$) between the functional groups and the mesoporous silica surface. It was the comprehensive interactions of CA with FMS that governed the CA orientation in FMS and the enzymatic activity performance. We believe that the enzymatic activity of CA in HOOC-FMS could be further improved by increasing P_{LD}, and optimizing the binding orientation via modifying FMS and/or re-engineering the CA's surface residues. Further work on covalently linking CA to NH_2-FMS is also ongoing in this lab. This work may provide a new approach converting carbon dioxide to biocarbonate in a biomimetic nanoconfiguration that can be integrated with the other part of biosynthesis process for the assimilation of carbon dioxide.

Acknowledgments

This work was supported by the NIH National Institute of General Medical Sciences (grant number R01GM080987) and the office of Basic Energy Sciences of US Department of Energy (award number KC020105-FWP12152) and the Transformational Materials Science Initiative of Pacific Northwest National Laboratory (PNNL). Wen Qi thanks the partially financial support from the China Scholarship Council. PNNL is operated for U.S. Department of Energy by Battelle under Contract DE-AC06-RLO1830.

References

1. Wigley TML, Richels R, Edmonds JA. Economic and environmental choices in the stabilization of atmospheric CO_2 concentrations. Nature. 1996; 379:240–243.
2. Aresta M, Quaranta E, Liberio R, Dileo C, Tommasi I. Enzymatic synthesis of 4-OH-benzoic acid from phenol and CO_2: the first example of a biotechnological application of a Carboxylase enzyme. Tetrahedron. 1998; 54:8841–8846.
3. Zevenhoven R, Eloneva S, Teir S. Chemical fixation of CO_2 in carbonates: Routes to valuable products and long-term storage. Catalysis Today. 2006; 115:73–79.

4. Berg IA, Kockelkorn D, Buckel W, Fuchs G. A 3-hydroxypropionate/4-hydroxybutyrate autotrophic carbon dioxide assimilation pathway in archaea. Science. 2007; 318:1782–1786. [PubMed: 18079405]
5. Huber H, Gallenberger M, Jahn U, Eylert E, Berg IA, Kockelkorn D, Eisenreich W, Fuchs G. A dicarboxylate/4-hydroxybutyrate autotrophic carbon assimilation cycle in the hyperthermophilic Archaeum Ignicoccus hospitalis. Proceedings of the National Academy of Sciences of the United States of America. 2008; 105:7851–7856. [PubMed: 18511565]
6. Field CB, Behrenfeld MJ, Randerson JT, Falkowski P. Primary production of the biosphere: integrating terrestrial and oceanic components. Science. 1998; 281:237–240. [PubMed: 9657713]
7. Price GD, Badger MR, Woodger FJ, Long BM. Advances in understanding the cyanobacterial CO_2-concentrating-mechanism (CCM): functional components, Ci transporters, diversity, genetic regulation and prospects for engineering into plants. J Exp Bot. 2008; 59:1441–1461. [PubMed: 17578868]
8. Davy R. Development of catalysts for fast, energy efficient post combustion capture of CO_2 into water; an alternative to monoethanolamine (MEA) solvents. Energy Procedia. 2009; 1:885–892.
9. SALLEY SO, SONG JY, WHITTLESEY GC, KLEIN MD. Thermal, Operational, and Storage Stability of Immobilized Carbonic Anhydrase in Membrane Lungs. ASAIO Journal. 1992; 38:M684–M687. [PubMed: 1457949]
10. Bond GM, Stringer J, Brandvold DK, Simsek FA, Medina M-G, Egeland G. Development of Integrated System for Biomimetic CO_2 Sequestration Using the Enzyme Carbonic Anhydrase. Energy & Fuels. 2001; 15:309–316.
11. Liu N, Bond GM, Abel A, McPherson BJ, Stringer J. Biomimetic sequestration of CO_2 in carbonate form: Role of produced waters and other brines. Fuel Processing Technology. 2005; 86:1615–1625.
12. Bhattacharya S, Schiavone M, Chakrabarti S, Bhattacharya SK. CO_2 hydration by immobilized carbonic anhydrase. Biotechnol Appl Biochem. 2003; 38:111–117. [PubMed: 12773097]
13. Ramanan R, Kannan K, Sivanesan S, Mudliar S, Kaur S, Tripathi A, Chakrabarti T. Bio-sequestration of carbon dioxide using carbonic anhydrase enzyme purified from Citrobacter freundii. World Journal of Microbiology and Biotechnology. 2009; 25:981–987.
14. Lindskog S. Structure and mechanism of carbonic anhydrase. Pharmacology & Therapeutics. 1997; 74:1–20. [PubMed: 9336012]
15. Breton S. The cellular physiology of carbonic anhydrases. Jop. 2001; 2:159–164. [PubMed: 11875253]
16. Minton AP. The Influence of Macromolecular Crowding and Macromolecular Confinement on Biochemical Reactions in Physiological Media. J Biol Chem. 2001; 276:10577–10580. [PubMed: 11279227]
17. Zhou H-X, Dill KA. Stabilization of proteins in confined spaces. Biochemistry. 2001; 40:11289–11293. [PubMed: 11560476]
18. Zhou HX. Protein folding and binding in confined spaces and in crowded solutions. Journal of Molecular Recongnition. 2004; 17:368–375.
19. Diaz JF, Balkus KJ Jr. Enzymes immobilized in MCM-41 molecular sieves. J Mol Catal B: Enzymatic. 1996; 2:115–126.
20. Gimon-Kinsel ME, Jimenez VL, Washmon LL, Balkus KJ Jr. Mesoporous molecular sieve immobilized enzymes. Stud Surf Sci Catal. 1998; 117:373–380.
21. Takahashi H, Li B, Sasaki T, Miyazaki C, Kajino T, Inagaki S. Catalytic activity in organic solvents and stability of immobilized enzymes depend on the pore size and surface characteristics of mesoporous silica. Chem Mater. 2000; 12:3301–3305.
22. Washmon LL, Balkus KJ Jr. Cytochrome c immobilized into mesoporous molecular sieves. J Mol Catal B: Enzymatic. 2000; 10:453–469.
23. Yiu HHP, Wright PA, Botting NP. Enzyme immobilisation using siliceous mesoporous molecular sieves. Microporous and Mesoporous Materials. 2001; 44–45:763–768.
24. Deere J, Magner E, Wall JG, Hodnett BK. Mechanistic and structural features of protein adsorption onto mesoporous silicates. J Phy Chem B. 2002; 106:7340–7347.

25. Han YJ, Stucky GD, Butler A. Mesoporous silicate sequestration and release of proteins. J Am Chem Soc. 1999; 121:9897–9898.
26. Lei C, Shin Y, Liu J, Ackerman EJ. Entrapping enzyme in a functionalized nanoporous support. J Am Chem Soc. 2002; 124:11242–11243. [PubMed: 12236718]
27. Lei C, Shin Y, Magnuson JK, Fryxell G, Lasure LL, Elliott DC, Liu J, Ackerman EJ. Characterization of Functionalized Nanoporous Supports for Protein Confinement. Nanotechnology. 2006; 17:5531–5538. [PubMed: 21727320]
28. Lei C, Shin Y, Liu J, Ackerman EJ. Synergetic Effects of Nanoporous Support and Urea on Enzyme Activity. Nano Letters. 2007; 7:1050–1053. [PubMed: 17341123]
29. Lei C, Soares TA, Shin Y, Liu J, Ackerman EJ. Enzyme Specific Activity in Functionalized Nanoporous Supports. Nanotechnology. 2008; 19:125102. [PubMed: 21817721]
30. Chen BW, Lei CH, Shin YS, Liu J. Probing mechanisms for enzymatic activity enhancement of organophosphorus hydrolase in functionalized mesoporous silica. Biochemical and Biophysical Research Communications. 2009; 390:1177–1181. [PubMed: 19874798]
31. Liu J, Shin Y, Nie ZM, Chang JH, Wang L-Q, Fryxell GE, Samuels WD, Exarhos GJ. Molecular assembly in ordered mesoporosity: A new class of highly functional nanoscale materials. J Phys Chem A. 2000; 104:8328–8339.
32. Feng X, Fryxell GE, Wang L-Q, Kim AY, Liu J, Kemner KM. Functionalized monolayers on ordered mesoporous supports. Science. 1997; 276:923–926.
33. Zhao DY, Feng JL, Huo QS, Melosh N, Fredrickson GH, Chmelka BF, Stucky GD. Triblock copolymer syntheses of mesoporous silica with periodic 50 to 300 angstrom pores. Science. 1998; 279:548–552. [PubMed: 9438845]
34. Liu J, Shin Y, Nie ZM, Chang JH, Wang L-Q, Fryxell GE, Samuels WD, Exarhos GJ. Molecular assembly in ordered mesoporosity: A new class of highly functional nanoscale materials. J Phys Chem A. 2000; 104:8328–8339.
35. Gitlin I, Gudiksen KL, Whitesides GM. Effects of Surface Charge on Denaturation of Bovine Carbonic Anhydrase. ChemBioChem. 2006; 7:1241–1250. [PubMed: 16847847]

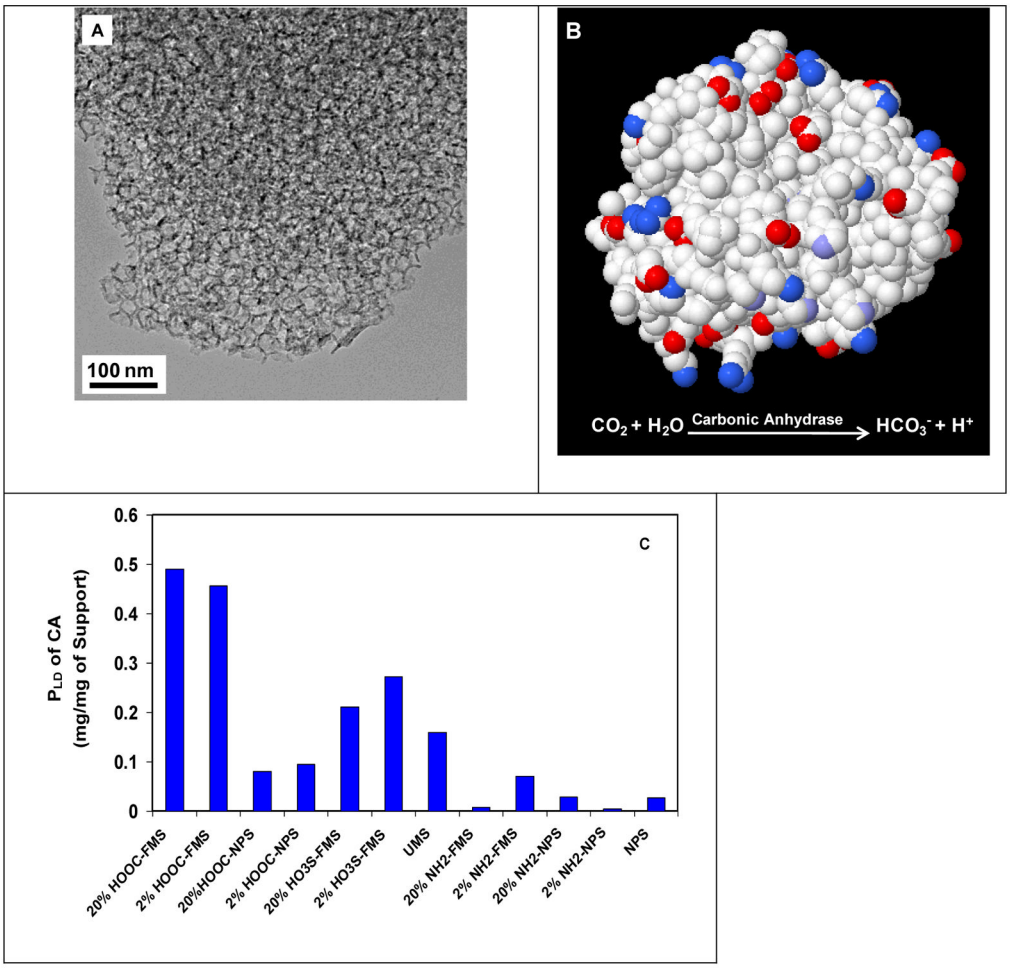

Figure 1.

(A) TEM image of 20% HOOC-FMS resulted from 20 nm UMS; (**B**) Protein structure of CA (PDB ID: 1V9E) with surface charge distribution (cationic-blue, anionic-red, uncharged-white); **(C)** Protein loading density of CA on various silica supports in H_2O at 21±1 °C.

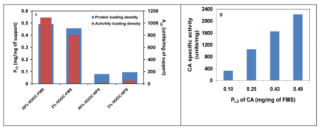

Figure 2.

(A) Specific activity and protein loading density of CA with 2% and 20% HOOC-FMS and HOOC-NPS in H_2O at 21±1 °C, respectively; **(B)** Specific activity of CA in 20% HOOC-FMS at various protein loading densities in H_2O at 21±1 °C. The specific activity of the free CA in H_2O was 3583.3 units/mg.

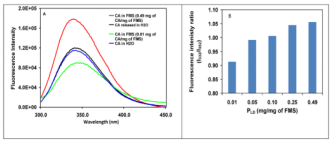

Figure 3.

(A) Fluorescence spectra of the free CA in H_2O, the entrapped CA in 20% HOOC-FMS, and the released CA from 20% HOOC-FMS in H_2O at 21±1 °C, where the baseline of the corresponding control sample (H_2O or FMS in H_20) was substracted. The released CA was prepared by first allowing CA released from FMS in pH 8.3, Tris-H_2SO_4 buffer, then dialysised in H_2O. [CA]: 0.02 mg/mL in H_2O. The specific activity of the free CA in H_2O was 3583.3 units/mg, while that of the released CA from HOOC-FMS was 3425.6 units/mg; (B) Fluorescence intenisty ratio at 332 and 352 nm (I_{332}/I_{352}) of CA in 20% HOOC-FMS at various loading densities.

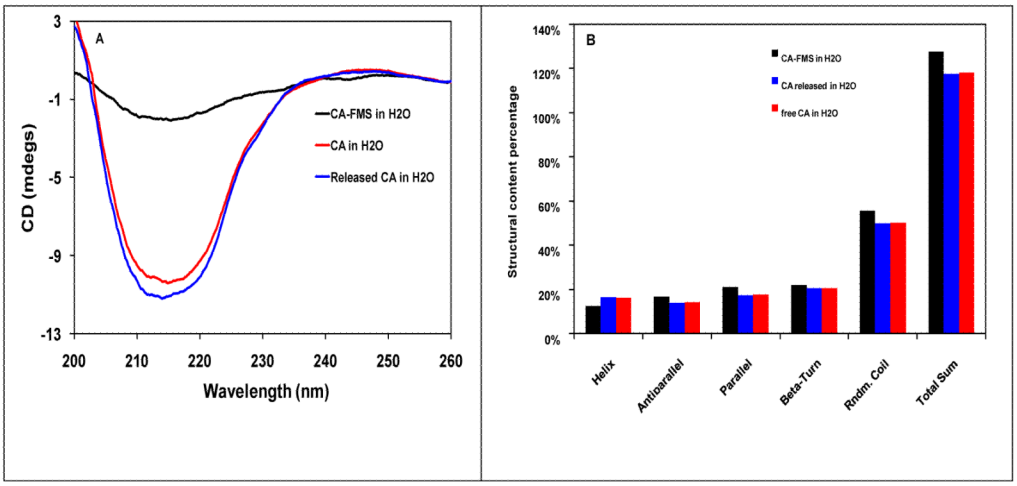

Figure 4.

(A) Circular dichroism spectra of the free CA in H_2O, the entrapped CA in 20% HOOC-FMS, and the released CA from 20% HOOC-FMS in H_2O at 25 °C, where the baseline of the corresponding control sample (H_2O or FMS in H_20) was substracted. The released CA was prepared by first allowing CA released from FMS in pH 8.3, Tris-H_2SO_4 buffer, then dialysised in H_2O. [CA]: 0.07 mg/mL in H_2O. The specific activity of the free CA in H_2O was 3583.3 units/mg, while that of the released CA from HOOC-FMS was 3425.6 units/mg; **(B)** Deconvolution results of CD spectra of CA and CA in 20% HOOC-FMS. Software used is CDNN 2.1. Analysis is based on CD spectra in the range of 200–260 nm.